arXiv:1611.05149v2 [q-bio.QM] 21 Nov 2016

Bridging the timescales of single-cell and population dynamics

Srividya Iyer-Biswas,[1,*] Herman Gudjonson,[2] Charles S. Wright,[1] Jedidiah Riebling,[1] Emma Dawson,[1,3] Klevin Lo,[4] Aretha Fiebig,[4] Sean Crosson,[4] and Aaron R. Dinner[2]

[1]*Department of Physics and Astronomy, Purdue University, West Lafayette, IN 47907*

[2]*James Franck Institute and Institute for Biophysical Dynamics, University of Chicago, Chicago, IL 60637*

[3]*Department of Physics, St Olaf College, Northfield, MN, 55057*

[4]*Department of Biochemistry and Molecular Biology, University of Chicago, Chicago, IL 60637*

Abstract

It is well known that population sizes increase exponentially during balanced growth. Concomitantly, at the single-cell level, the sizes of individual cells themselves increase exponentially; the single-cell exponential growth-rate also determines the statistics of cell size and cell division time distributions. Seeking an integrated perspective of microbial growth dynamics under balanced conditions, we formulate a theoretical framework that takes into account observables at both single-cell and population scales. Our exact analytical solutions for both symmetric and asymmetric cell division reveal surprising effects of the stochastic single-cell dynamics on features of population growth. In particular, we find how the population growth rate is sensitive to the shape of the distribution of cell division times. We validate the model by quantitatively predicting the observed cell-age distributions without fitting parameters. Our model also provides a prescription for deducing the time for transitioning from the swarmer (reproductively quiescent) to stalked (reproduction able) stage of the *C. crescentus* lifecycle; our predictions match with previous indirect estimates. We discuss the scalings of all timescales with external parameters that control the balanced growth state. For *C. crescentus* cells, we show that the rate of exponential growth of single (stalked) cells governs the dynamics of the entire lifecycle, including the swarmer-to-stalked cell transition.

* iyerbiswas@purdue.edu

I. INTRODUCTION

The earliest quantitative microbiology experiments revealed that microbial population sizes increase exponentially in favorable conditions [1]. Similar dynamics are also observed (to a good approximation) in the population growth of other species, the spreading of pandemics, the polymerase chain reaction for amplification of DNA fragments, global internet traffic increase, multiplication of viruses in T cells, and tumor growth [2]. There are unifying themes in the quantitative characterizations of exponential growth in these different contexts, codified in general results of the theory of branching processes [3, 4]. However, the idiosyncrasies of each experimental system determine the important dynamical variables and measurables in that specific context. For instance, in demographic studies the age structure of the human population in a region at a given time can be well characterized. However, there is typically a paucity of data for the total population number over multiple human lifespans. Thus indirect estimation of the Malthusian parameter (the exponential growth rate) from the observed age structures is a focus of these studies [5].

In contrast, in standard bulk-culture bacterial growth studies, the dynamical range in the population number of cells can be readily made to span multiple logarithmic decades in a day or two, since the typical timescales involved are of the order of minutes. Thus precise estimation of the exponential growth rate, k, defined to be the inverse of the time taken for the numbers of cells to increase by a factor of e, is feasible in this context [2]. Since many kinds of cells divide precisely into two cells at each division, the bulk growth rate is often used to infer the cell doubling time, i.e., the time it takes for a *single* cell to fission into two daughter cells, using the formula $(\ln 2)/k$ [2]. However, the extrapolation from the observed growth rate of the population (typically involving $\mathcal{O}(10^8)$ cells per ml) to the inferred dynamics at the single-cell level is often inaccurate because all cells do not divide at precisely the same time after birth. There is significant stochasticity in the division times (also known as generation times, cell lifetimes, interdivision times, or waiting times)—typically the COV (the coefficient of variation, defined as the ratio of the standard deviation to the mean) of division times is $10-30\%$ [6–18]. One must account for this variability in relating the stochastic single-cell division dynamics to the population growth; even the mean population growth rate depends on the *shape* of the

division time distribution.

A unique advantage of studying balanced exponential growth in the microbial context is that high quality data are accessible at multiple scales of observation (sub-cellular, organismal and population level). In particular, the technology that we have recently developed for *C. crescentus* cells has the advantage that isolated single-cells in highly reproducible and unlimiting balanced-growth conditions can be observed with unprecedented statistical precision [6]; complementary approaches have been introduced by others for other organisms. Thus direct comparison between these single-cell experiments and bulk-culture measurements under the same growth conditions is possible. Here we develop a theory of microbial growth dynamics under balanced growth conditions and demonstrate its use for integrating data from both single-cell and bulk-culture measurements of *C. crescentus* cells to make specific predictions at both scales.

A special feature of *C. crescentus* cells is that they divide asymmetrically: a stalked cell grows and divides into two distinct daughter cells: another stalked cell and a swarmer cell, which has to undergo an additional differentiation step before it transitions into a reproduction-capable stalked cell. The division and differentiation steps are thus controlled by distinct stochastic waiting-time distributions (see Fig. 1). Therefore, we generalize the theory to include asymmetric division and derive a prescription for inferring this additional timescale (swarmer-to-stalked cell transition time) from the combination of population and single-cell data. Using our results, we examine scalings of all timescales with external parameters that control the balanced growth state. We combine these results to show how a simple measurement of the population growth rate in a given condition reveals the statistics of stochastic growth and division of individual cells under these conditions.

II. RESULTS

System characterization and notation. Since the number of cells per ml in typical bulk-culture measurements is very large (e.g., $\mathcal{O}(10^8)$), we can treat the total number of cells in the population at a time t, $N(t)$, as a continuous variable. Moreover, it is reasonable to assume that the fluctuations in $N(t)$ relative to its mean value are negligible. In asymptotic balanced growth, $N(t)$ is expected to grow exponentially, i.e., $N(t) = N(0)\exp(k\,t)$.

Here, k denotes the exponential growth rate of population size; it can be experimentally obtained from standard bulk-culture measurements. We denote the age of the cell, i.e., the time since the last division, by τ; $P(\tau)d\tau$ is the probability that a cell lives to age τ and then divide between ages τ and $\tau + d\tau$. In contrast, the division *propensity*, $\alpha(\tau)$, is defined as follows: $\alpha(\tau)d\tau$ is the probability that a given cell of age τ divides between τ and $\tau+d\tau$. One might be tempted to equate it to $P(\tau)$, but the two are distinct and related as follows: $\alpha(\tau) = P(\tau)/\left[1 - \int_0^\tau d\tau' P(\tau')\right]$ (see SI for details). We note that in balanced growth, the division time distribution, $P(\tau)$, is independent of the time of observation, t. In microbial systems, the number of progeny per cell is typically a constant number (a positive integer, such as 1 or 2); we denote it by ν. We define the age-dependent number density, $n(t,\tau)$, as follows: $n(t,\tau)d\tau$ is the number of cells present at t, with ages between τ and $\tau + d\tau$. In this paper we consider growth conditions in which the probability of cell-mortality is negligible. Thus the total number of cells (and so the number of cells of each age) increases indefinitely. Mathematically, being in balanced growth state means that the *fraction* of cells of each age at any time, t, is time invariant. Therefore, the cell-age distribution, $G(t,\tau) \equiv n(t,\tau)/N(t)$, is time-independent in the long time (balanced growth) limit. We denote this steady-state age distribution by $G^*(\tau)$. It is a normalized probability density since the sum of fractions of cells at each age is unity. In practice, single-cell measurements yield $P(\tau)$, from which the division propensity, $\alpha(\tau)$, can be computed (see above). Thus, the question then becomes how, given $P(\tau)$ and ν, the corresponding population exponential growth rate, k, and the age distribution, $G^*(\tau)$, are to be self-consistently determined.

General solution for symmetric cell-division. To place the general solution in context, it is useful to first consider two familiar limiting cases of the problem. (i) In the *deterministic* limit, cells divide exactly at age τ_o, i.e, $P(\tau) = \delta_{\tau,\tau_o}$. Therefore, $N(t) = N(0)\,\nu^{(t/\tau_o)}$. Here, when $\nu = 2$, the doubling time is equal to the division time, τ_o. (ii) When the the dynamics are *Markovian* or memoryless, the division time distribution is an exponential, $P(\tau) = \kappa\, e^{-\kappa\tau}$. The dynamics in this case are identical to those of a one-step stochastic Hinshelwood cycle [19], or equivalently, an age-dependent Galton-Watson process with an exponential waiting-time distribution [3]. The full solution is known; in particular, $N(t) = N(0)\, e^{\kappa t}$. Thus the population growth rate, k, is equal to the single-cell exponential waiting time distribution parameter, κ. Note that even for this simple case, the mean

division time of single cells, $\mu_\tau = 1/k$, is not equal to the mean doubling time of the population, $(\ln 2)/k$.

In general, the propensity of a cell to divide depends on its age, i.e., α varies with τ. Consequently, the time evolution is non-Markovian, and $P(\tau)$ is non-exponential. This significantly increases the complexity of the problem of finding the population growth rate, k, as a functional of $P(\tau)$; for symmetric division, the process falls in the category of a Bellman-Harris branching process [3]. Typically, the division time distribution is a unimodal distribution with a positive skew, i.e., it has a long right tail and is thus qualitatively different from the monotonically decreasing exponential distribution (Markovian limit). Therefore solving the general non-Markovian case is important. We derive the time evolution equations for the age-dependent number density, $n(t,\tau)$, and the age distribution, $G(t,\tau)$, for a general $P(\tau)$ and solve them exactly (see **Methods** and SI).

In the general case, the population's exponential growth rate, k, is related to the single-cell division time distribution, $P(\tau)$, through the integral

$$\left\langle e^{-k\tau} \right\rangle_P \equiv \int_0^\infty d\tau\, e^{-k\tau} P(\tau) = \frac{1}{\nu}. \tag{1}$$

In words, k is the point at which the Laplace transform of the division time distribution, $P(\tau)$, is equal to $1/\nu$. The expressions for the age distribution and the total population number, for a given initial condition, $N(0)$, are

$$\begin{aligned} G^*(\tau) &= \frac{\nu k}{(\nu-1)} e^{-k\tau} \left[1 - \int_0^\tau d\tau' P(\tau') \right]; \\ N(t) &= N(0)\, e^{k t}; \\ n(t,\tau) &\equiv N(t)\, G^*(\tau) = N(0) \frac{\nu k}{(\nu-1)} e^{-\left[\int_0^\tau d\tau' \alpha(\tau')\right]}. \end{aligned} \tag{2}$$

Together, Eqs. (1) and (2) constitute the complete analytical solution to the problem for symmetric cell division.

From the general solution it follows that there is a unique steady-state age distribution, $G^*(\tau)$, corresponding to a given division time distribution, $P(\tau)$, and progeny number, ν. Conversely, if the (population) cell-age distribution and the bulk exponential growth rate are observed, Eq. (2) can be used to infer the *single-cell* division time distribution! We note that the growth rate, k, is itself a functional of $P(\tau)$ for a given ν, and is thus not an independent parameter of the solution for $G^*(\tau)$ in Eq. (2).

Since the shape of the age distribution reveals features of the division time distribution, its qualitative features are of interest. Briefly, they are as follows. (See Fig. S1 for a graphical summary of these results.) First, the age distribution monotonically decreases with τ. To see this, note that in Eq. (2), the cumulative integral $\int_0^\tau d\tau' P(\tau')$ increases with τ since $P(\tau) > 0$. Next, since $P(\tau) \propto d\left(e^{k\tau} G^*\right)/d\tau$, the most probable division time is determined by where the curvature of $e^{k\tau} G^*(\tau)$ changes sign, i.e., its point of inflection. Also note that the slope of this function at its point of inflection estimates the width of the division time distribution. For $\nu = 1$, a case considered in detail below, the mean division time is given by the point of inflection of the age distribution and the slope at this point estimates the width of the division time distribution. Finally, for a given $P(\tau)$, a greater value of ν (number of progeny per cell) will increase the growth rate and skew the age distribution towards smaller ages (i.e., to the left).

Comparison with single-cell experiments: measured and predicted cell-age distributions. We compare our theory to recent single-cell data for *C. crescentus* [6]. *C. crescentus* divides into two morphologically and functionally distinct daughter cells: an adherent stalked cell that is replication competent and a motile swarmer cell that cannot divide further but can differentiate into a stalked cell. In these microfluidic experiments [6], stalked cells are retained and swarmer cells are removed after each division (see Fig. 1 and SI for more information). Therefore the stalked-cell dynamics (in these experimental conditions) are equivalent to cells being simply "renewed" after each division, i.e., $\nu = 1$. Also, the total number of stalked cells in the experiment, $N(t)$, is constant. These features simplify the problem, and we can use the analytical results for the symmetric-division model. However, the growth dynamics are still non-Markovian and hence non-trivial. For $\nu = 1$ the relation between the division time and age distributions becomes

$$G^*(\tau) = \frac{1}{\mu_\tau}\left[1 - \int_0^\tau d\tau' P(\tau')\right], \tag{3}$$

where μ_τ is the mean division time, $\mu_\tau \equiv \int_0^\infty d\tau\, \tau P(\tau)$. See SI for details and Fig. S1 for a graphical interpretation.

We use the measured time-courses of single-cell growth and division to validate the theory as follows. We obtain the *measured* cell-age distribution by building a histogram of the duration between the time of observation and the recorded time of the previous division for each cell. From the same experiment, we also measure the division time

distribution, and we insert it into Eq. (3) to compute the *predicted* age-distribution. For experiments spanning the physiological temperature range of the organism, we find excellent agreement between the measured and predicted cell-age distributions with no fitting parameters (Fig. 2A), confirming the model.

When rescaled by their condition-specific means, cell-age distributions from all temperatures collapse onto a single curve (Fig. 2B symbols). The underlying physical principle encoded in this universal behavior is that a single temperature-dependent scale of time, proportional to the mean division time (or equivalently, the mean age), governs stochastic growth and division dynamics [6, 19]. For the scaling collapse of the corresponding mean-rescaled division time distributions see [6].

We note that the mean age, μ_a, and mean division time, μ_τ, are not equal. For $\nu = 1$, using Eq. (3), the two are related by

$$\mu_a = \frac{\mu_\tau}{2}\left(1 + \eta_\tau^2\right), \tag{4}$$

where η_τ is the COV of the $P(\tau)$ distribution. Using Eqs. (3) and (4), we find the predicted mean-rescaled age distribution; this also agrees excellently with the observed distribution (Fig. 2B line). Eq. (4) shows that when there is no stochasticity in division times (i.e., the deterministic case $P(\tau) = \delta_{\tau,\tau_o}$), then the mean age is half the mean division time since cell age is uniformly distributed from 0 to τ. Interestingly, this provides a lower bound for the mean age (for a specified mean division time) since any stochasticity in $P(\tau)$ can only increase η_τ, and thus the mean age. We note that in practice, even if there is sizable noise in division times, the second term is negligible compared to the first (for 20% noise in division times, the ratio of the two terms is 0.04). Thus, $\mu_a \approx \mu_\tau/2$.

Once the age distribution (for a specific balanced growth condition) has been determined, it can be used to deconvolve cell-cycle phase dependence from a population of asynchronous cells, since it predicts the probability weight to associate with cells of each age. This obviates the need for less precise bulk-synchronization experiments, in which it is also unclear how the synchronization procedure may itself alter the balanced growth state. For instance, if the initial population has only swarmer cells, then the numbers of stalked and swarmer cells in the population oscillate with time and the culture is far from being in balanced growth (Fig. 4). We note that an early empirical algorithm for cell-cycle phase deconvolution was given in [20].

Generalization to asymmetric division. Motivated in part by the *C. crescentus* data discussed above, we now generalize the theory to allow for asymmetric divisions (see Fig. 1). There are two distinct cell types in the population: normal division-capable cells, and reproductively quiescent cells which take an additional stochastic waiting time, T_q, to differentiate (transition) to normal cells before being able to divide. Each normal cell divides into ν normal cells and ν_q quiescent cells. The waiting time T_q has probability distribution $P_q(T_q)$. Normal cells divide with a division time distribution, $P(\tau)$, as before. With the inclusion of asymmetric division, the process is no longer a standard branching process, since different cells in the population are not statistically identical [21]. This significantly increases the complexity of the problem. However, we have found exact analytical solutions (see **Methods** and SI). We denote the (steady-state) age distributions of normal and quiescent cells by $G^*(\tau)$ and $G_q^*(T_q)$, respectively. In the $\nu_q = 0$ limit the problem becomes equivalent to the symmetric division case.

A key physical insight is that the ratio of normal to quiescent cells should be a constant for balanced growth conditions. Consequently, both kinds of cells must increase exponentially in numbers, with the *same* growth rate, k. See **Methods** and SI for details. The exact solution for k, for specified functional forms of $P(\tau)$ and $P_q(T_q)$, when ν normal and ν_q quiescent progeny are born at each division, is

$$\left\langle e^{-k\tau}\right\rangle_P = \frac{1}{\nu + \nu_q \left\langle e^{-kT_q}\right\rangle_{P_q}}. \tag{5}$$

In this solution $\left\langle e^{-k\tau}\right\rangle_P \equiv \int_0^\infty d\tau P(\tau)e^{-k\tau}$ and $\left\langle e^{-kT_q}\right\rangle_{P_q} \equiv \int_0^\infty dT_q\, P_q(T_q)e^{-kT_q}$. For the complete solution, including expressions for $G^*(\tau)$, $G_q^*(T_q)$, and the fixed ratio of stalked to swarmer cells, see SI.

Comparison with population level experiments: scaling of timescales in the *C. crescentus* lifecycle. For *C. crescentus* cells, the "normal" cell stage corresponds to stalked cells, and "quiescent" cells are identified with swarmer cells. Each stalked cell divides into a stalked cell and a swarmer cell. The swarmer differentiates into a stalked cell after a time, T_q. Thus, for bulk-culture experiments with *C. crescentus* cells, $\nu = \nu_q = 1$, and Eq. (5) becomes

$$\left\langle e^{-k\tau}\right\rangle_P = \frac{1}{1 + \left\langle e^{-kT_q}\right\rangle_{P_q}}. \tag{6}$$

From our bulk-culture experiments, we are able to determine the population growth rate, k (see **Methods** for details). Moreover, $P(\tau)$ is also known, since it is directly observed in our single-cell experiments. Thus, the timescale that remains to be determined is the swarmer-to-stalked cell transition time, T_q, and the corresponding distribution, $P_q(T_q)$. There are several technical reasons why direct experimental characterization of T_q is challenging (see [22]). Yet knowledge of this timescale could provide an important clue to many fundamental biological questions. For example, it is not known precisely what fraction of the *C. crescentus* lifecycle is spent in the swarmer stage. Determining this may in turn indicate how the additional differentiation step in the lifecycle confers flexibility to the fitness of *C. crescentus* cells in different growth conditions. Also, results in [6] imply that there must be cell size growth at the swarmer stage, since the average size of a newborn swarmer is only $\approx 80\%$ of the average size of a newborn stalked cell, and the newborn stalked cell size distribution has been shown to be invariant. But whether swarmer cell sizes increase linearly, exponentially, or in a rapid growth spurt during differentiation, remains to be determined.

Here we estimate the swarmer-to-stalked transition time for different balanced growth conditions using Eq. (6). The results are shown in Fig. 3. At each growth condition, we invert the (integral) equation to estimate T_q, using the experimentally determined k (the bulk growth rate) and $P(\tau)$ (the stalked cell division time distribution). The mean value of this timescale, μ_{T_q}, is insensitive to the particular functional form assumed for $P_q(T_q)$. Therefore, we use $P_q(T_q) = \delta(T_q - \mu_{T_q})$ and find μ_{T_q} using Eq. (5), after numerically evaluating the Laplace transform for $P(\tau)$ at k for each growth condition. Remarkably, the *fraction* of the cell cycle spent in the swarmer stage is a constant, as temperature is varied (and the duration of the lifecycle itself changes by a factor of ≈ 4). Specifically, we find that $\mu_\tau k = 0.6$ and $\mu_{T_q} = 0.4\mu_\tau$ (Fig. 3). This result is consistent with indirect measurements in [22]. Moreover, using this ratio, we can predict the ratio of swarmer to stalked cells in the population during balanced growth (see SI for details). We find that $N_q(t)/N(t) \approx 0.2$, also consistent with previous estimates [22], further validating our approach.

In [6] we showed that the *single-cell* exponential growth rate (of stalked cell sizes), k_{sc}, determines a condition-specific cellular unit of time. Thus, it governs all aspects of the stochastic dynamics of stalked-cell growth and division; in particular, its inverse is pro-

portional to the mean division time, μ_τ, and it also determines the full distribution, $P(\tau)$. Since we now find that μ_{T_q}/μ_τ is also a constant, the implication is that the single-cell exponential growth time scale, k_{sc}^{-1}, proportional to the population growth rate, k, governs all relevant timescales for growth, division *and differentiation*. Thus *all* timescales rescale proportionally, when external conditions are changed (see Fig. 3). The remarkable implication is that for any balanced growth condition of interest, a simple measurement of the population growth rate, k, when used to rescale the universal mean-rescaled distributions we have found (Fig. 2 and [6]), together with the model, yields distributions of cell-division times, cell ages, and cell sizes.

Moreover, we find that the population and single-cell exponential growth rates are approximately equal to each other for all temperatures in Fig. 3: $k_{sc} \approx k$. The surprising implication of this observation is that the duration of the swarmer-to-stalked cell transition time is accounted for by the fact that cell numbers *double* in the time that cell sizes increase by a factor of 1.8. This observation is consistent with swarmer cell sizes also increasing exponentially with time, with the same growth rate. However, this interpretation is speculative at this time.

Numerical simulations: scaling of fluctuations in population numbers. To extend the results to transient population growth dynamics (before the balanced growth state is attained), to examine fluctuations in population numbers, and to confirm the analytical predictions, we performed stochastic simulations for population growth for different waiting-time distributions and progeny numbers. We developed an exact algorithm for simulating these non-Markovian population growth dynamics (see SI for details). We note that the standard Gillespie algorithm [23] cannot be used, since it assumes exponential waiting-time distributions. Our simulation results are summarized in Fig. 4. Interestingly, in the transient phase, the numbers of normal (stalked) and quiescent (swarmer) cells oscillate with time. Thus the ratio of population numbers of swarmers to stalked cells also oscillates before reaching the analytically predicted steady-state value. The mean-rescaled distributions of numbers of swarmer and stalked cells undergo a striking scaling collapse, similar to the one observed for the stochastic Hinshelwood cycle model [19], suggesting that this scaling collpase is a universal signature of coupled stochastic exponential growth.

III. CONCLUDING REMARKS

In summary, we have related single-cell division to population growth, by introducing an analytical framework that takes dynamics at both scales into account. We have validated this framework by matching predicted and observed age distributions for *C. crescentus* cells in balanced growth at different conditions. We have also used this framework to show how timescales characterizing these dynamics scale with external conditions (different temperatures), and shown that a single timescale governs all aspects of these dynamics.

In this work we have identified the cell age distribution, $G(\tau)$, as an important "order parameter" for describing the non-equilibrium steady-state of cells in balanced growth conditions. The analytical framework introduced here could also provide a starting point for examining transient responses to changes in external conditions in different contexts: for instance, following a temperature change, a nutritional shift or a chemical perturbation to molecular regulators of cell cycle progression. Evidently, the *functional* change of the age-distribution characterizes the transient dynamics following the perturbation. In future work, we will explore these transient responses by extending the approach introduced here.

IV. METHODS

Here we briefly indicate how we wrote down and solved the time evolution equations for the age distribution and the age-dependent number density. For the symmetric case, consider the fraction of cells between ages τ and $d\tau$ at a time, t: $G(t,\tau)d\tau$. After a small interval of time dt elapses, the fraction of cells in each age interval changes due to two distinct processes, aging and division. Newborn cells always appear at $\tau = 0$. Accounting for these probabilities gives the time evolution equation for the age distribution. For asymmetric division, there are three distinct processes that evolve the stalked and swarmer cell age distributions: aging, division and differentiation. In analogy with the symmetric case, we write the coupled time evolution equations for the age distributions of the normal and quiescent cells. See SI for details of derivation and solution. The exact algorithm we have developed to simulate the stochastic non-Markovian population

growth dynamics is detailed in the SI.

The single-cell data are those presented in [6]. Population growth data were obtained using standard optical density measurements. For each experimental condition 12–20 growth curves were obtained under dilute growth conditions; for each growth curve we recorded 6–10 data points in the "log–phase". The exponential growth rate of the population was determined by averaging the growth rates obtained from the log phase data of each growth curve.

V. ACKNOWLEDGMENTS

We thank Steve Berry, Rudro Biswas, Jon Henry, Norbert Scherer, Michael Vennettelli, and Tom Witten for useful discussions, and Farshid Jafarpour for a careful reading of the manuscript. We thank Purdue University Startup Funds, Purdue Research Foundation, and the National Science Foundation (NSF REU grant PHY-1460899, NSF PHY-1305542, and NSF DBI-1300426) for financial support.

VI. AUTHOR CONTRIBUTIONS

SI-B conceived of and designed research; SI-B developed the theoretical model in consultation with ARD, performed analytical calculations, and observed scaling behaviors reported; HG and JR performed simulations and tested models under the guidance of ARD and SI-B; CSW performed image and data analyses; ED and KL performed bulk-culture measurements under the guidance of SI-B and AF; SI-B and SC provided reagents and biological supplies; SI-B, CSW, JR and ARD wrote the paper.

---

[1] J. Monod, Annu. Rev. Microbiol. 3, 371 (1949).

[2] S. J. Hagen, Am. J. Phys. 78, 1290 (2010).

[3] W. Feller, *An introduction to probability theory and its applications* (John Wiley & Sons, 2008).

[4] M. Kimmel and D. E. Axelrod, "Branching processes in biology," (2002).

[5] H. R. Thieme, *Mathematics in population biology* (Princeton University Press, 2003).

[6] S. Iyer-Biswas, C. S. Wright, J. T. Henry, K. Lo, S. Burov, Y. Lin, G. E. Crooks, S. Crosson, A. R. Dinner, and N. F. Scherer, PNAS 111, 15912 (2014).

[7] T. M. Norman, N. D. Lord, J. Paulsson, and R. Losick, Annu. Rev. Microbiol. 69, 381 (2015).

[8] G. Lambert and E. Kussell, Phys. Rev. X 5, 011016 (2015).

[9] K. S. Korolev, J. B. Xavier, and J. Gore, Nat. Rev. Cancer 14, 371 (2014).

[10] K. C. Huang, D. W. Ehrhardt, and J. W. Shaevitz, Curr. Opin. Microbiol. 15, 707 (2012).

[11] H. Salman, N. Brenner, C.-k. Tung, N. Elyahu, E. Stolovicki, L. Moore, A. Libchaber, and E. Braun, Phys. Rev. Lett. 108, 238105 (2012).

[12] D. Siegal-Gaskins and S. Crosson, Biophys. J. 95, 2063.

[13] T. J. Strovas, L. M. Sauter, X. Guo, and M. E. Lidstrom, J. Bacteriol. 189, 7127 (2007).

[14] S. D. Talia, J. M. Skotheim, J. M. Bean, E. D. Siggia, and F. R. Cross, Nature 448, 947 (2007).

[15] Y. Wakamoto, J. Ramsden, and K. Yasuda, Analyst 130, 311 (2005).

[16] E. Powell, Biometrika 42, 16 (1955).

[17] C. Kelly and O. Rahn, J. Bacteriol. 23, 147 (1932).

[18] T.-Y. Lin, T. M. Santos, W. S. Kontur, T. J. Donohue, and D. B. Weibel, J. Bacteriol. 197, 3446 (2015).

[19] S. Iyer-Biswas, G. E. Crooks, N. F. Scherer, and A. R. Dinner, Phys. Rev. Lett. 113, 028101 (2014).

[20] D. Siegal-Gaskins, J. N. Ash, and S. Crosson, PLoS Comput. Biol. 5, e1000460 (2009).

[21] N. Van Kampen, *Stochastic processes in physics and chemistry*, 3rd ed. (North Holland, 2007).

[22] J. C. England, B. S. Perchuk, M. T. Laub, and J. W. Gober, J. Bacteriol. 192, 819 (2010).

[23] D. T. Gillespie, J. Phys. Chem. 81, 2340 (1977).

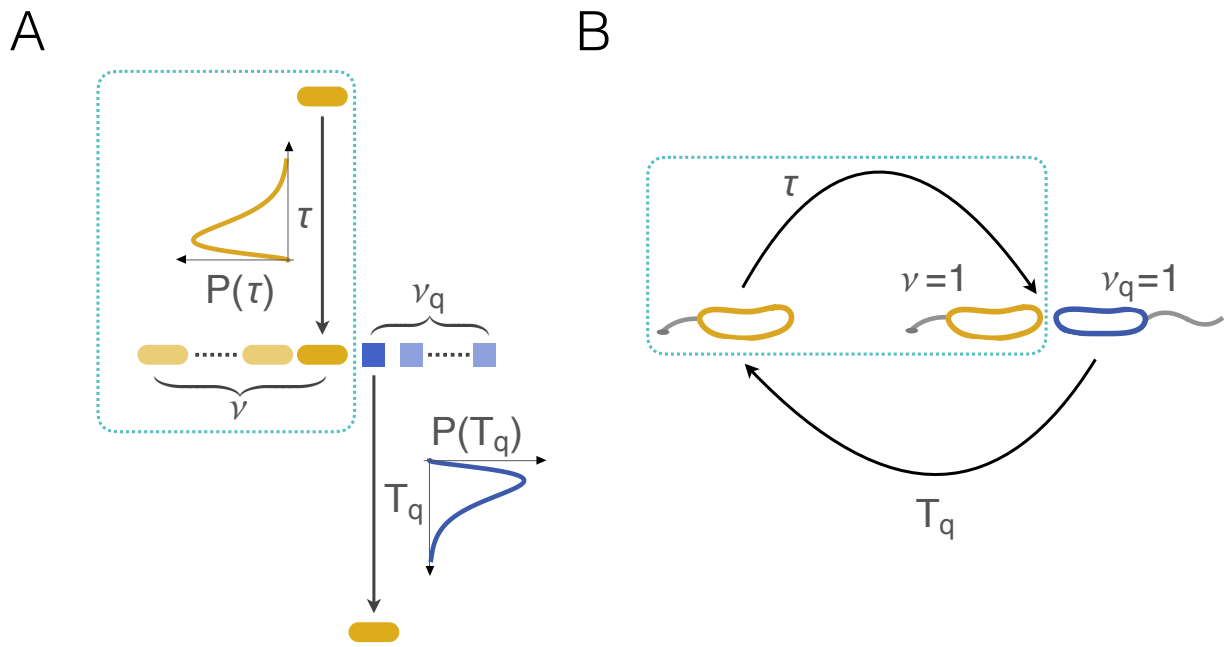

FIG. 1. **Schematic representation of model and experimental system.** In (A) we summarize the general model considered. Upon division, a normal (yellow) cell divides into ν normal cells and ν_q reproductively quiescent (blue) cells. Division occurs after a stochastic waiting time τ, drawn from a distribution, $P(\tau)$. The quiescent cells transition into normal cells with a waiting-time distribution, $P_q(T_q)$. Model specification requires knowledge of $\nu, \nu_q, P(\tau)$ and $P_q(T_q)$. By setting $\nu_q = 0$ one obtains a model of symmetric division (dotted cyan box). In (B) we show a schematic of the relevant timescales in the *C. crescentus* lifecycle: the stalked (normal) cell division time, τ, and the swarmer (quiescent) cell to stalked cell transition time, T_q. Upon division a stalked cell gives birth to a stalked and a swarmer cell. Thus the *C. crescentus* cell-cycle reduces to the model in (A) with $\nu = \nu_q = 1$. The single-cell technology introduced in [6] corresponds to a model with $\nu = 1$ and $\nu_q = 0$ (dotted cyan box).

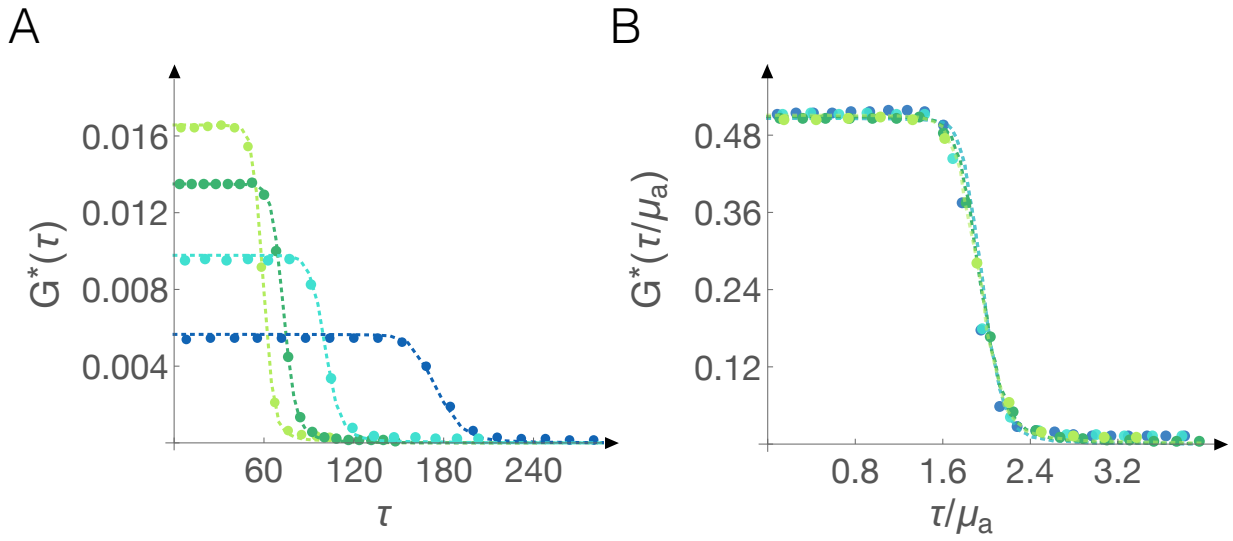

FIG. 2. **Cell age distributions, measured and predicted, from different temperatures.** In (A) we show the age distributions from different temperatures (light green, 34°C; dark green, 31°C; cyan, 24°C; and blue, 17°C). The data from single-cell experiments are shown with circular symbols and the predictions from the theory (with no adjustable parameters) are shown with corresponding dashed lines. In (B) we show the same distributions as in (A), rescaled by their respective temperature dependent mean ages; evidently, they undergo a scaling collapse, consistent with a single condition-specific timescale dominating stochastic growth and division statistics (see text).

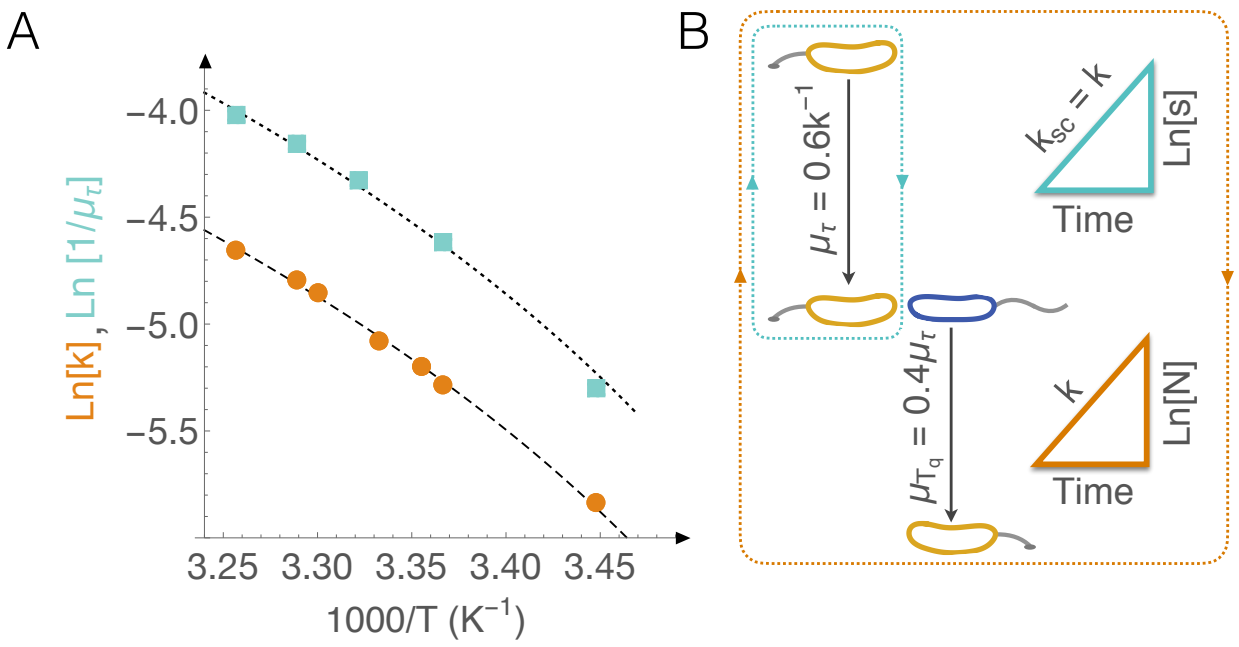

FIG. 3. **Scaling of timescales in the *C. crescentus* lifecycle.** (A) The population growth rate, k (orange circles), and the single-cell mean division rate from[6] (cyan squares) are shown as functions of temperature on an Arrhenius plot. The measurement precision is better than the sizes of the plot markers. The dotted (dashed) line is the best fit Ratkowsky curve [6] for the single-cell (population) data. Both fits are found to be proportional to each other, with Ratkowsky temperature 269 K; by finding the ratio of the two curves, we find that $\mu_\tau k = 0.6$. (B) Combining the results from (A) with Eq. (6) and results from [6], we are able to characterize all timescales in the *C. crescentus* lifecycle as fractions of mean single-cell division time, or equivalently, the inverse of the population growth rate (see accompanying text). At different temperatures all timescales change proportionally. s and N denote the cell size and the population size, respectively. k_{sc} is the exponential growth rate of individual-cell size, s (cyan triangle) and k is the exponential growth rate of total population number, N (orange triangle). Observables at the population and individual-cell levels are respectively shown in orange and cyan. Single-cell measurements sample the dynamics of stalked cell division (cyan rectangle), whereas population growth measurements sample the dynamics of stalked cell division and swarmer cell differentiation (orange rectangle).

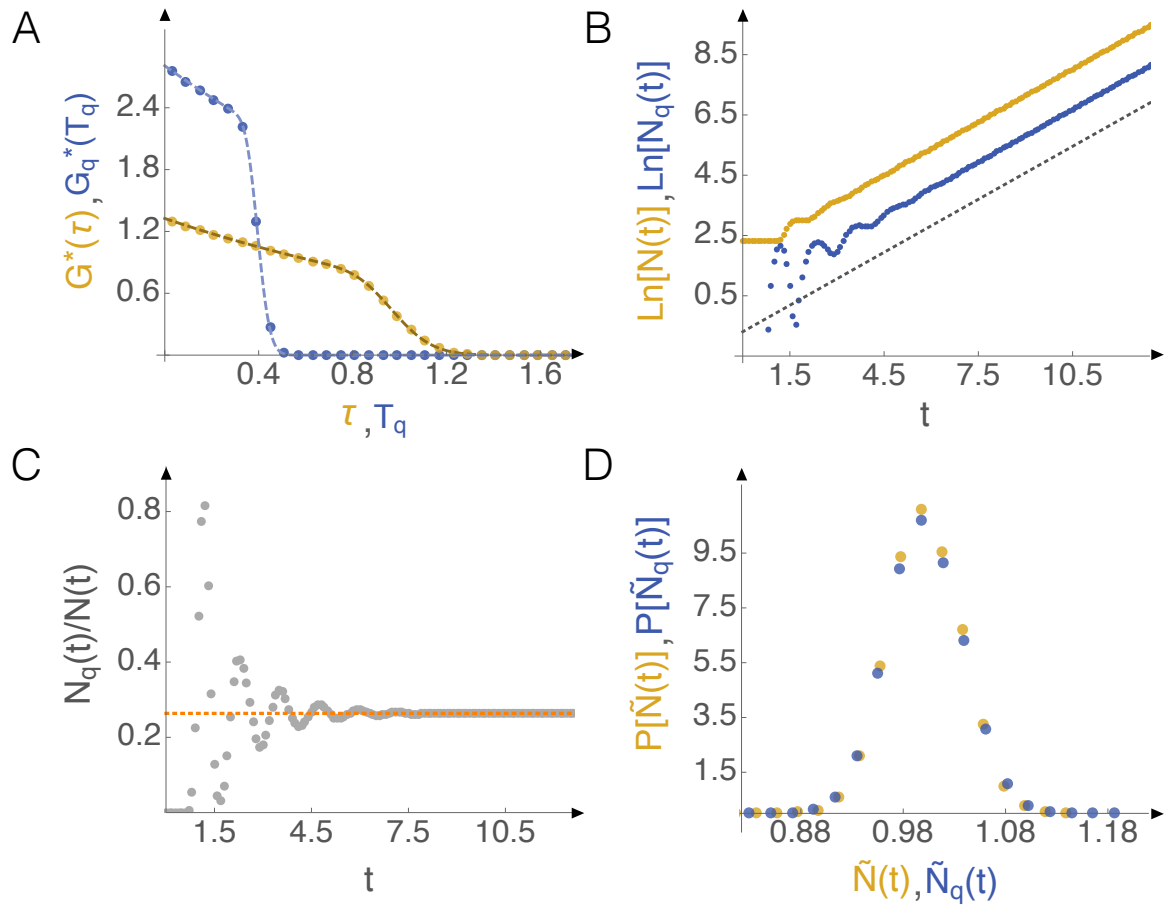

FIG. 4. **Simulation results for stochastic population growth.** In (A) we show that the numerically simulated age distributions (dotted data) for normal (yellow) and quiescent (blue) cells match model predictions (dashed lines). In (B), we show simulation results for the exponential increase in population sizes of normal (yellow) and quiescent (blue) cells. In steady-state, they have the same exponential growth rate, which is accurately predicted by the analytical solution (dashed line). Oscillations in numbers of normal and quiescent cells are observed during the transient phase. In (C), the ratio of quiescent to normal cells matches with the steady-state analytical prediction (dashed orange line), and also oscillates during initial transient dynamics. In (D) we show that the mean-rescaled population number distributions of normal and quiescent cells (from $t = 10$ in panel (C)) undergo a scaling collapse. Here, $\tilde{N}(t) = N(t)/\langle N(t)\rangle$ and $\tilde{N}_q(t) = N_q(t)/\langle N_q(t)\rangle$. The parameter values used for these simulations are: $\nu = \nu_q = 1$; $N(0) = 10$; $N_q(0) = 0$; $P(\tau)$ is a Gamma distribution with mean = 1 and COV = 0.13 and $P_q(T_q)$ is a Gamma distribution with mean = 0.4 and COV = 0.1. All timescales are measured in units of μ_τ.

Supplemental Information

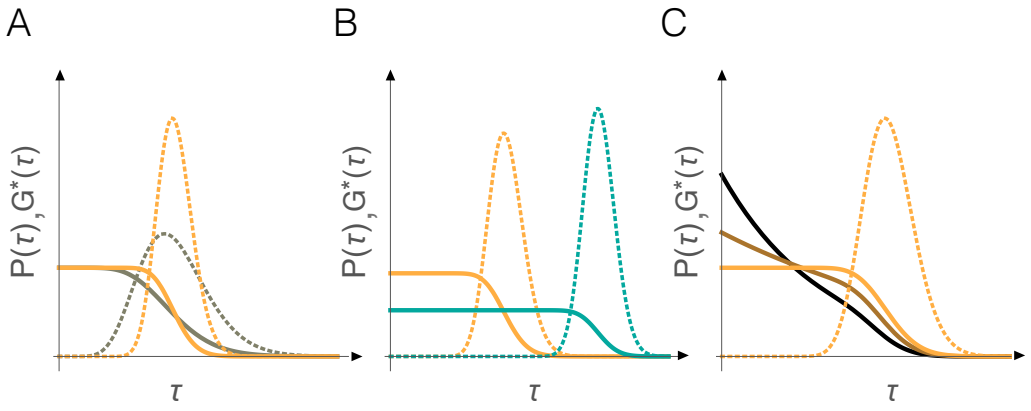

Supplementary Figure S1. **Relation between the division time distribution, $P(\tau)$, and the steady-state age distribution, $G^*(\tau)$, for a given progeny number, ν.** See main text, Eqs. (1), (2) and (3) and accompanying text, for explanation of symbols and discussion of results. In (A) we have shown cell-age distributions (bold orange and gray curves) for $\nu = 1$ corresponding to two $P(\tau)$ distributions (dotted orange and gray); the $P(\tau)$ distributions have the same mean but different COVs. The figure illustrates that the point of inflection of the cell-age distribution determines the mean division time and the slope at the point of inflection determines the width of the division time distribution. In (B) we have shown cell-age distributions (bold orange and cyan) for $\nu = 1$, corresponding to two $P(\tau)$ distributions (dotted orange and cyan) which have the same COV but different means. Evidently, the point of inflection of $G^*(\tau)$ predicts the mean division time. In (C) we show age distributions for $\nu = 1$ (bold orange), $\nu = 2$ (brown) and $\nu = 5$ (black) for the same division time distribution (dotted orange).

I. ANALYTICAL METHODS

A. Case 1: Symmetric division

Definitions.

- t denotes the observation time.
- τ denotes the age of the cell measured from the time since it last divided.

- $n(t,\tau)d\tau \equiv$ number of cells at time t with ages between τ and $\tau + d\tau$.
- $N(t) \equiv \int_0^\infty d\tau\, n(t,\tau) \equiv$ total number of cells present at time t.
- $G(t,\tau) \equiv n(t,\tau)/N(t)$. Thus, $G(t,\tau)d\tau \equiv$ the fraction of cells at time t with ages between τ and $\tau + d\tau$.
- $\alpha(\tau)$, the division propensity, is probability that a cell of age between τ and $\tau + d\tau$ will divide in the interval $d\tau$. Note that by construction $\alpha(\tau)$ is independent of t.
- $P(\tau)d\tau \equiv$ the probability that a cell does not divide up until τ and then divides between τ and $\tau + d\tau$. Therefore, $P(\tau)d\tau =$ [the probability that a cell does not divide until τ]$\times\alpha(\tau)d\tau = \left[1 - \int_0^\tau d\tau' P(\tau')\right]\alpha(\tau)d\tau$. Thus, $\alpha(\tau) = P(\tau)/\left[1 - \int_0^\tau d\tau' P(\tau')\right]$.

Time evolution equations for the age distribution.

Aging of cells and cell-division events result in temporal evolution of $n(t,\tau)$:

$$\begin{aligned} & n(t+dt,\tau)d\tau = n(t,\tau - dt)d\tau - \alpha(\tau)dt\, n(t,\tau - dt)d\tau \\ \implies & n(t+dt,\tau) - n(t,\tau) = -n(t,\tau) + n(t,\tau - dt) - \alpha(\tau)dt\, n(t,\tau - dt) \\ \implies & \partial_t n(t,\tau) = -\partial_\tau n(t,\tau) - \alpha(\tau)n(t,\tau). \end{aligned} \tag{S-1}$$

The products of cell division, ν per cell, appear as new 'just-born' $\tau = 0$ members of the cell population. Accounting for this contribution to the age group $0 < \tau < dt$, between times t and $t + dt$, one has

$$n(t,0) = \nu\left[\int_0^\infty d\tau n(t,\tau)\alpha(\tau)\right] \equiv \nu\rho(t)N(t). \tag{S-2}$$

$\rho(t)$, as defined above, is the cell-averaged rate at which newborn cells result across the entire cell population, while $\alpha(\tau)$ is the propensity of birthing new cells at time τ.
Now, for $\nu > 1$, cell numbers will increase exponentially and thus will not reach a 'steady state'. However, we expect the age distribution, $G(t,\tau) = n(t,\tau)/N(t)$, to have a steady state in all realistic cases. Therefore the goal is to find its time-evolution equation. In order to achieve this, we first find the total population growth rate, using Eqns. (S-1) and (S-2):

$$\begin{aligned} \partial_t N(t) &= \int_0^\infty (\partial_t n(t,\tau))\, d\tau = n(t,0) - n(t,\infty) - \int_0^\infty d\tau n(t,\tau)\alpha(\tau) \\ &= (\nu - 1)\,\rho(t)N(t). \end{aligned} \tag{S-3}$$

The time evolution equation for $G(t,\tau)$ is obtained by differentiating both sides of the identity $n(t,\tau) = G(t,\tau)N(t)$ with respect to t, and then using Eqns. (S-1), (S-2) and (S-3):

$$\begin{aligned} &\partial_t n(t,\tau) = N(t)\partial_t G(t,\tau) + G(t,\tau)\partial_t N(t), \\ \Rightarrow\ &-\partial_\tau n(t,\tau) - \alpha(\tau)n(t,\tau) = N(t)\partial_t G(t,\tau) + G(t,\tau)\,(\nu-1)\,\rho(t)N(t). \end{aligned} \tag{S-4}$$

Dividing throughout by $N(t)$, we obtain the time evolution equation of the age distribution:

$$\partial_t G(t,\tau) + \partial_\tau G(t,\tau) + \alpha(\tau)G(t,\tau) + (\nu-1)\,\rho(t)G(t,\tau) = 0. \tag{S-5}$$

We can account for newborn daughter cells by dividing Eq. (S-2) by $N(t)$:

$$G(t,0) = \nu\left[\int_0^\infty d\tau\, G(t,\tau)\alpha(\tau)\right] \equiv \nu\rho(t). \tag{S-6}$$

Steady state solution.

In steady state the age distribution, $G(t,\tau)$, and consequently the birth-rate, $\rho(t)$, will both be time-independent. These steady-state quantities, denoted by the superscript '*', satisfy t-independent versions of Eqs. (S-5) and (S-6):

$$\partial_\tau G^*(\tau) + [\alpha(\tau) + (\nu-1)\,\rho^*]\,G^*(\tau) = 0, \tag{S-7a}$$

$$G^*(0) = \nu\left[\int_0^\infty d\tau\, G^*(\tau)\alpha(\tau)\right] \equiv \nu\rho^*. \tag{S-7b}$$

From Eq. (S-3) we have

$$\begin{aligned} &\partial_t N(t) = (\nu-1)\,\rho^* N(t) \equiv kN(t), \\ \Rightarrow\ &N(t) = N(0)e^{kt}. \end{aligned} \tag{S-8}$$

Thus, as expected, the total cell population grows exponentially with the rate

$$k = (\nu-1)\,\rho^*. \tag{S-9}$$

Defining $A(\tau) \equiv \int_0^\tau d\tau'\alpha(\tau')$ and using the above relation between k and ρ^*, Eq. (S-7) becomes

$$\frac{d}{d\tau}\left[G^*(\tau)\,e^{k\tau + A(\tau)}\right] = 0. \tag{S-10}$$

Integrating both sides from $\tau' = 0$ to $\tau' = \tau$, and using Eq. (S-6),

$$G^*(\tau)\, e^{k\tau + A(\tau)} = G^*(0) = \nu \rho^* = \frac{k\nu}{\nu - 1}. \tag{S-11}$$

Thus, the steady state age distribution is

$$G^*(\tau) = \frac{k\nu}{\nu - 1}\, e^{-k\tau} e^{-A(\tau)}. \tag{S-12}$$

When $\nu > 1$, the only unknown number in this expression, k, may be found from the normalization of the probability density, $G^*(\tau)$:

$$1 = \int_0^\infty d\tau\, G^*(\tau) = \frac{k\nu}{\nu - 1} \int_0^\infty d\tau\, e^{-k\tau} e^{-A(\tau)}. \tag{S-13}$$

Using the relation $P(\tau) = \alpha(\tau) e^{-A(\tau)}$, which follows from the definitions of $\alpha(\tau)$ and $A(\tau)$, the normalization equation for G^* becomes

$$\int_0^\infty d\tau P(\tau) e^{-k\tau} \equiv \langle e^{-k\tau} \rangle_P = \frac{1}{\nu}. \tag{S-14}$$

When $\nu = 1$, system is closed, since the total number of cells is conserved. For this case, since $N(t)$ is a constant, ρ is a constant, and a simplification of the previous general derivation is obtained. Therefore Eq. (S-7) can be directly integrated to compute the normalized steady-state age distribution for $\nu = 1$:

$$G^*(\tau) = 1 - \frac{1}{\mu_\tau} \int_0^\tau d\tau' P(\tau'), \tag{S-15}$$

where the mean value, μ_τ, is evaluated w.r.t. the division time distribution, $P(\tau)$.

B. Case 2: Asymmetric division

Time evolution equations for the age distributions of normal and quiescent cells.

The cell population now has two distinct cell types: normal reproducing cells, and quiescent cells which transition to normal cells before they can divide. The normal cells divide with propensity $\alpha(\tau)$ at age τ, creating ν normal and ν_q quiescent cells. Their division time distribution is $P(\tau) = \alpha(\tau) e^{-A(\tau)}$, where $A(\tau) = \int_0^\tau \alpha(\tau') d\tau'$. Thus, these terms are defined just as we did for the symmetric case. The quiescent cells are similarly defined, transitioning to normal cells with propensity $\alpha_q(T_q)$ and with a corresponding

waiting time distribution $P_q(T_q) = \alpha_q(T_q)e^{-A_q(T_q)}$, where $A_q(T_q) = \int_0^{T_q} \alpha_q(T_q')\,dT_q'$. Using the subscript q to denote the quantities defined for the quiescent cells, the time evolution equations for the number density of cells with age τ are:

$$\partial_t n(t,\tau) = -\partial_\tau n(t,\tau) - \alpha(\tau)n(t,\tau), \tag{S-16a}$$

$$\partial_t n_q(t,T_q) = -\partial_{T_q} n_q(t,T_q) - \alpha_q(T_q)n_q(T_q). \tag{S-16b}$$

Newborn cells result from cell division of normal cells, as well as from the conversion of quiescent to normal cells:

$$n(t,0) = \nu N(t)\rho(t) + N_q(t)\rho_q(t), \tag{S-17a}$$

$$n_q(t,0) = \nu_q N(t)\rho(t). \tag{S-17b}$$

Analogous to the symmetric case, the per-cell division and conversion rates, ρ and ρ_q, are defined as follows:

$$\rho(t) = \int_0^\infty d\tau \frac{n(t,\tau)}{N(t)}\alpha(\tau) = \int_0^\infty d\tau\, G(t,\tau)\alpha(\tau), \tag{S-18a}$$

$$\rho_q(t) = \int_0^\infty dT_q \frac{n_q(t,T_q)}{N_q(t)}\alpha_q(T_q) = \int_0^\infty dT_q\, G_q(t,\tau_q)\alpha_q(\tau_q). \tag{S-18b}$$

Combining these equations yields the time evolution equations for total population numbers $N(t)$ and $N_q(t)$:

$$\partial_t N = (\nu - 1)N\rho + N_q\rho_q, \tag{S-19a}$$

$$\partial_t N_q = \nu_q N\rho - N_q\rho_q. \tag{S-19b}$$

1. *Steady state solution.*

After a sufficiently long time, we expect the age distributions G and G_q, and thus the cell-averaged division and conversion rates, respectively ρ and ρ_q, to stabilize and become time independent. Below we consider only this long time steady state limit of these quantities, and as such we discard the previous use of the superscript '$*$' in this context. For later use, we define the following (constant) ratio in steady state:

$$\gamma = \frac{\rho_q}{\rho}. \tag{S-20}$$

In steady state we expect both cell population numbers to grow exponentially with the *same* rate k:

$$\frac{\partial_t N(t)}{N(t)} = \frac{\partial_t N_q(t)}{N_q(t)} = k, \quad \Rightarrow \quad N(t), N_q(t) \propto e^{kt}. \tag{S-21}$$

From this, it is clear that the following ratio must become time-independent:

$$\phi = \frac{N_q(t)}{N(t)}. \tag{S-22}$$

Eqns. (S-19), (S-20) and (S-22) can be combined to yield the following steady state equations:

$$\frac{\partial_t N(t)}{N(t)} = \rho\,(\nu + \phi\gamma - 1), \tag{S-23a}$$

$$\frac{\partial_t N_q(t)}{N_q(t)} = \rho\left(\frac{\nu_q - \phi\gamma}{\phi}\right). \tag{S-23b}$$

Comparing these with Eq. (S-21), we find

$$\frac{k}{\rho} = \nu + \phi\gamma - 1 = \frac{\nu_q - \phi\gamma}{\phi}. \tag{S-24}$$

Combining Eqs. (S-16), (S-17) and (S-21), we can write down the equations satisfied by the age distributions G and G_q in steady state:

$$\partial_\tau G(\tau) + [k + \alpha(\tau)]\, G(\tau) = 0, \tag{S-25a}$$

$$\partial_\tau G_q(\tau) + \Big[k + \alpha_q(\tau)\Big] G_q(\tau) = 0. \tag{S-25b}$$

The initial conditions are, respectively, $G(0) = \rho(\nu + \phi\gamma)$ and $G_q(0) = \rho\nu_q/\phi$. These equations are then solved to obtain the expressions:

$$G(\tau) = \rho(\nu + \phi\gamma) e^{-k\tau} e^{-A(\tau)}, \;\; A(\tau) = \int_0^\tau \alpha(\tau')\, d\tau', \tag{S-26a}$$

$$G_q(T_q) = \frac{\rho\nu_q}{\phi} e^{-kT_q} e^{-A_q(T_q)}, \qquad A_q(T_q) = \int_0^{T_q} \alpha_q(T_q')\, dT_q'. \tag{S-26b}$$

Normalizing the two distributions G and G_q, analogous to the symmetric case above, we find:

$$\langle e^{-k\tau} \rangle_P = 1 - \frac{k}{\rho(\nu + \phi\gamma)} = \frac{1}{\nu + \phi\gamma}, \tag{S-27a}$$

$$\langle e^{-kT_q} \rangle_{P_q} = 1 - \frac{k\phi}{\rho\nu_q} = \frac{\gamma\phi}{\nu_q}. \tag{S-27b}$$

To derive these equations we have used Eq. (S-24). Eliminating $\gamma\phi$ from these equations, we find the equation (analogous to Eq. (S-14) for the symmetric case) which determines the growth rate, k:

$$\langle e^{-k\tau}\rangle_P = \frac{1}{\nu + \nu_q \langle e^{-kT_q}\rangle_{P_q}}. \tag{S-28}$$

Using this in Eq. (S-27), one can determine the value of $\phi\gamma$. These, combined with Eq. (S-24), yield the individual values of ρ, ϕ and γ, thus solving the full steady state problem.

II. NUMERICAL METHODS

Algorithm for stochastic population growth simulations.

We developed exact stochastic population growth simulations in order to numerically validate and extend our analytical results. We aim to computationally investigate stochastic dynamics of population growth, namely the expansion of population number and evolution of the population age distribution in time. Since our growth models are generally non-Markovian, the current state of the system during a simulation cannot be simply summarized by aggregate statistics. Instead, we need to efficiently track individual waiting times for each simulation constituent to produce accurate trajectories. In these simulations, we model cell division and changes in cell state (see main text) with arbitrary waiting time distributions. During the course of a run, each cell is individually accounted for in time. Our implementation can be succinctly summarized as follows. (1) For each cell present, we probabilistically generate the time (from the provided waiting distributions) at which that cell will either divide or change state, if that has not yet been determined. (2) We then choose the most immediate event and perform it on the associated cell. If the cell divides, we replace it with two new cells; if the cell changes state, we modify its corresponding attribute. (3) We then update the current time and repeat until the desired time or population is reached. As the simulation progresses, we successively record any desired statistics, including population size and cell ages.

By explicitly identifying the time of the next cell event (Step 2), we ensure that our simulations progress in natural time order. Since cells are statistically independent, an al-

ternative viable strategy would be to simply process cell events in an arbitrary order until all cells reach the desired simulation end time. While maintaining a natural ordering increases the computational cost of simulation by a factor $\mathcal{O}(\log(N))$, we believe it has a few advantages. With this configuration, we can condition individual runs on first-passage type statistics and naturally accommodate interactions between cells in future applications. In addition, we only need to maintain the current population of cells during simulation, rather than maintaining the full record of all past events.